

Breaking the bonds of generative artificial intelligence by minimizing the maximum entropy

Mattia Miotto¹ and Lorenzo Monacelli²

¹Center for Life Nanoscience, Istituto Italiano di Tecnologia, Viale Regina Elena 291, 00161, Rome, Italy

²Department of Physics, Sapienza University, Piazzale Aldo Moro 5, 00185, Rome, Italy

The emergence of generative artificial intelligence (GenAI), comprising large language models, text-to-image generators, and AI algorithms for medical drug and material design, had a transformative impact on society. However, despite an initial exponential growth surpassing Moore’s law, progress is now plateauing, suggesting we are approaching the limits of current technology. Indeed, these models are notoriously data-hungry, prone to overfitting, and challenging to direct during the generative process, hampering their effective professional employment.

To cope with these limitations, we propose a paradigm shift in GenAI by introducing an *ab initio* method based on the minimal maximum entropy principle. Our approach does not fit the data. Instead, it compresses information in the training set by finding a latent representation parameterized by arbitrary nonlinear functions, such as neural networks. The result is a general physics-driven model, which is data-efficient, resistant to overfitting, and flexible, permitting to control and influence the generative process.

Benchmarking shows that our method outperforms variational autoencoders (VAEs) with similar neural architectures, particularly on undersampled datasets. We demonstrate the method’s effectiveness in generating images, even with limited training data, and its unprecedented capability to customize the generation process *a posteriori* without the need of any fine-tuning or retraining.

Generative artificial intelligence (GenAI) refers to models capable of algorithmically producing – novel – data resembling those from the training set. Text generative models, for instance, predict the probability of each possible next token, *i.e.* clusters of characters, of a sequence to generate a plausible continuation of an initial prompt [1].

Multiple algorithms have been developed for such tasks, each offering distinct advantages depending on the data type. For instance, transformers are particularly effective for sequence generation, as seen in large language models [2], while Generative Adversarial Networks (GANs) [3], Variational Autoencoders (VAEs) [4], and Diffusion models [5] are well-suited for handling multidimensional data, such as images. Thanks to these models/architectures, GenAI is being used to address a wide range of complex problems [6], from designing drugs [7, 8] and functional proteins[9] to the discovery of novel materials [10], from advertising and entertainment [11] to education [12] and communication [13].

Parallel to the enormous spreading of GenAI, serious ethical concerns regarding the generated content are being formulated [14], and the feasibility of further improving by just scaling existing architectures is questioned [15]. Indeed, the extremely data-greedy nature of most GenAI models is leading to a saturation of the available data [15], while training with generated samples is demonstrated to poison the models [16, 17]. In addition, GenAI models tend to overfit [14], verbatim memorizing entire parts of the training set [18], with consequential ethical concerns about the generated content closely resembling copyright-protected items or personal data [19, 20].

With some remarkable exceptions, most GenAI solutions struggle to find a transformative impact. While

these models can rapidly generate novel samples, customizing the results remains challenging, often requiring multiple, supervised random attempts to steer the outcome [21, 22]. Considerable efforts have been revolved to mitigate this issue [21–26], that still relies on model-specific solutions, requiring *ad hoc* retraining each time the underlying model is updated.

Our work introduces a paradigm shift to GenAI that addresses these limitations by proposing a novel method based on the ‘minimal maximum entropy’ principle.

I. THE MINIMAL MAXIMUM ENTROPY PRINCIPLE

Maximum entropy is a guiding principle to assign probabilities to events [27]. Indeed, maximizing entropy selects the most unbiased probability distribution consistent with given constraints, ensuring no unwarranted assumptions are made beyond the available information. Given a set of measures $f_i(x)$, the probability distribution that (i) maximizes entropy and (ii) ensures that the expected values of f_i match those observed in the training set, is given by:

$$\tilde{P}_{f_i, \lambda_i}(x) = \frac{1}{Z} \exp \left[- \sum_i \lambda_i f_i(x) \right], \quad (1)$$

with $Z = \int dx \exp[-\sum_i \lambda_i f_i(x)]$. Here, the integral marginalize over all possible configurations x and λ_i are Lagrange multipliers that constrain the average values of

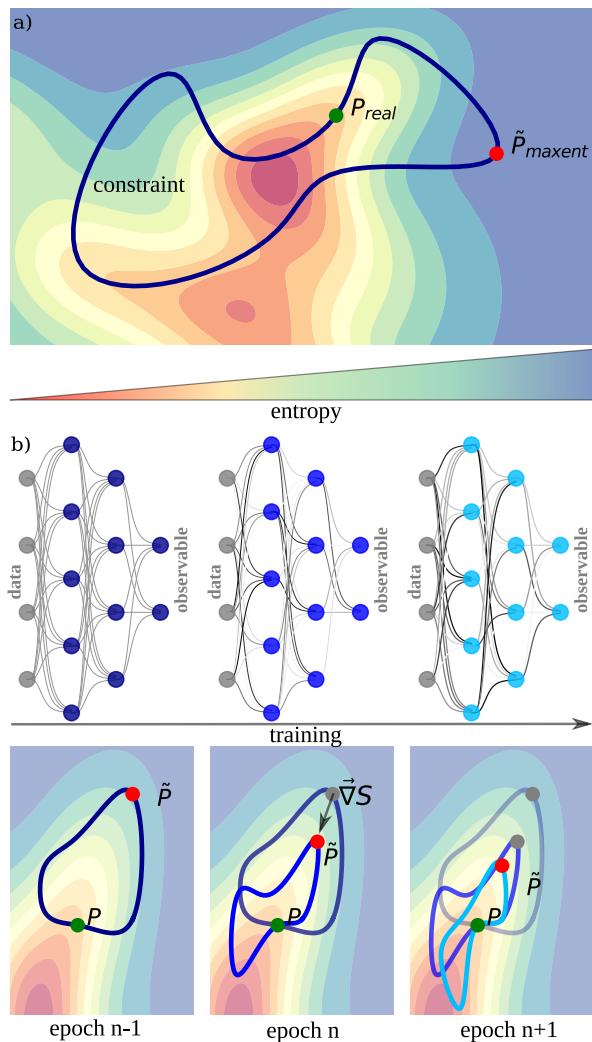


FIG. 1: **Illustration of the minimal maximum entropy principle.** **a)** Two dimensional representation of a possible entropy landscape as a function of two reaction coordinates, with a dark blue line marking the values of the entropy subject to a given constraint/observable. Colors shift from red to blue as the entropy increases. Green and red dots identify the real and maximum entropies values, respectively. **b)** The observables/constraints can be defined in an unsupervised way using a neural network to extract the relevant features from the input data. Starting from a fully connected network with equal weights, the minimal maximum entropy algorithm adjusts the network parameters to obtain the constraint whose associated maximum entropy is minimum, i.e. closer to the real entropy.

the measures $f_i(x)$ to match those of the training set.

$$\int dx f_i(x) \frac{1}{Z} \exp \left[- \sum_i \lambda_i f_i(x) \right] = \frac{1}{N} \sum_{\{x\}_{\text{train set}}} f_i(x) = \mu_i. \quad (2)$$

Operationally, training a maximum entropy model consists of the following steps: i) define a set of measures $f_i(x)$, ii) compute the average values μ_i of such

measures on the training dataset, iii) solve iteratively Eq. (2) to find the values of λ_i . Once we got the converged λ_i values, the maximum entropy principle ensures that the entropy of the target $\tilde{P}_{f_i, \lambda_i}(x)$ is always above the exact entropy [28]. Since both the real probability distribution, $P(x)$, and the MaxEnt one $\tilde{P}_{f_i, \lambda_i}(x)$ satisfy the constraints $\int dx f_i(x) P(x) = \mu_i$, they belong to the same manifold of all the distributions satisfying $\langle f_i(x) \rangle = \mu_i$, where $\langle \cdot \rangle$ indicates the expected value (sketched in Figure 1a). $\tilde{P}_{f_i, \lambda_i}(x)$ maximizes the entropy within this manifold, thus, $S[\tilde{P}_{f_i, \lambda_i}]$ is always higher or equal to the real distribution Shannon's entropy $S[P]$: $S[\tilde{P}_{f_i, \lambda_i}] \geq S[P]$.

The inequality between real and MaxEnt entropy sets up a new variational principle: for a fixed set of measures f_i , the entropy of the corresponding MaxEnt distribution is always above the real one. The residual entropy difference quantifies how much information can be further extracted from the data by improving the choice of $f_i(x)$.

From the minimal maximum entropy principle, we can introduce a Min-MaxEnt algorithm to optimize the set of measures f_i by minimizing the entropy of the MaxEnt distribution $S[\tilde{P}_{f_i, \lambda_i}]$:

$$S[P] = \min_{f_i} S[\tilde{P}_{f_i, \lambda}] \quad (3)$$

The equality in Eq. (3) holds as it always exists a set of measures f_i that uniquely define a probability distribution [28]. In practice, the measures f_i can be parametrized as generic nonlinear functions of the configurations, depending on a vector of parameters $\theta_1, \dots, \theta_n$ (see Figure 1), and the minimization of the entropy can be performed directly optimizing $\theta_1, \dots, \theta_n$:

$$\tilde{P}[\{\theta_i\}_1^n, \{\lambda_i\}_1^n](x) = \frac{1}{Z} \exp \left[- \sum_i \lambda_i f_i[\theta_1, \dots, \theta_n](x) \right] \quad (4)$$

Therefore, we must simultaneously train the λ_i parameters to constrain the averages of f_i (Eq. 2), and the θ_i parameters to minimize the maximum entropy (Eq. 3). To optimize λ_i , we define a cost function quantifying the displacement of the f_i averages between training and generated samples [28, 29]:

$$\chi^2 = \sum_i \frac{(\langle f_i \rangle - \mu_i)^2}{\sigma_i^2} \quad (5)$$

where σ_i^2 is the variance of the i -th observable on the training dataset. The minimization of Eq. (5) can be preconditioned as discussed in Ref. [28]. The parameters λ_i are updated with a gradient descent algorithm according to

$$\lambda_i \longrightarrow \lambda_i - \eta \frac{\partial \chi^2}{\partial \lambda_i} \quad (6)$$

(In this work, we employed the ADAM algorithm [30]). Next, we introduce an update rule also for the θ_i parameters that decrease the maximum entropy. As sketched in

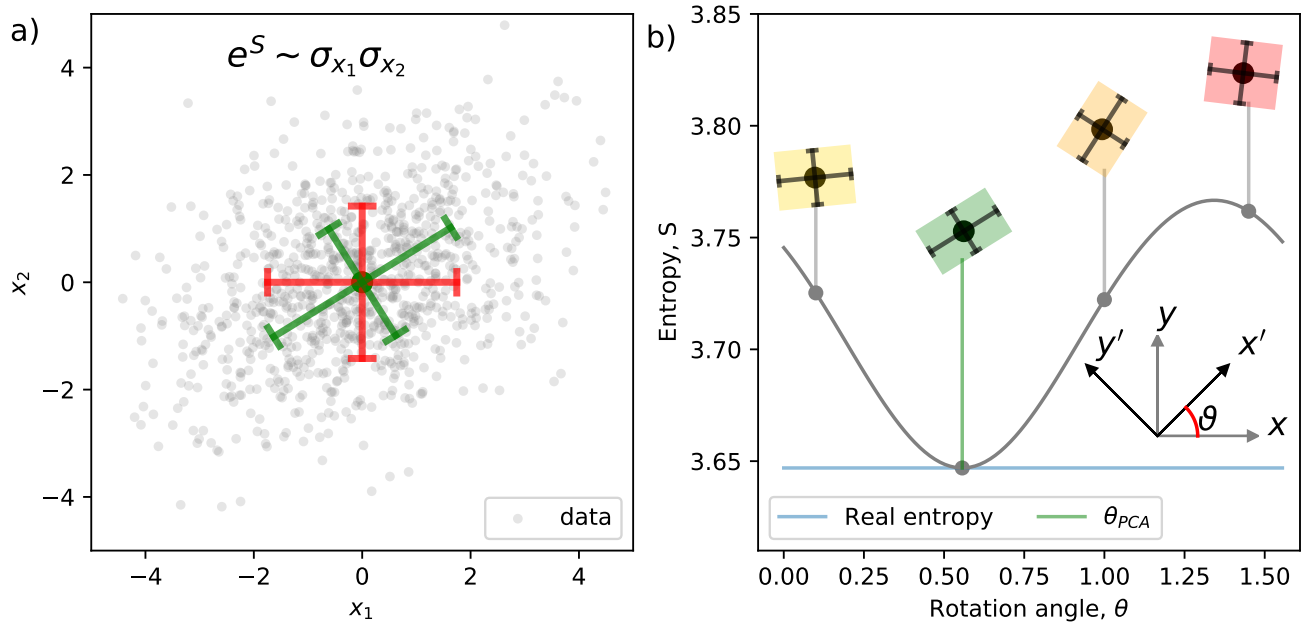


FIG. 2: **Principal component analysis as a special Min-MaxEnt solution.** **a)** Example of 2D normal distributed data. Red and green bars represent the squared roots of the variances in two different basis. **b)** Entropy as a function of the rotation angle of the basis in which data are represented.

Figure 1b, updating $\theta_1 \cdots \theta_n$ progressively modifies the constraint manifold, minimizing the entropy of the corresponding MaxEnt distribution. This is achieved by computing the gradient of the MaxEnt distribution's entropy

$$\theta_i \longrightarrow \theta_i - \eta \frac{dS}{d\theta_i}. \quad (7)$$

Notably, the entropy itself is practically incomputable. However, the entropy gradient is a standard observable and can be evaluated efficiently as:

$$\frac{dS}{d\theta_i} = - \sum_j \lambda_j \left(\left\langle \frac{df_j}{d\theta_j} \right\rangle_{\tilde{P}[\theta_1, \dots, \theta_n, \lambda_1, \dots, \lambda_n]} - \left\langle \frac{df_j}{d\theta_j} \right\rangle_P \right), \quad (8)$$

where $\left\langle \frac{df_j}{d\theta_j} \right\rangle_{\tilde{P}[\theta_1, \dots, \theta_n, \lambda_1, \dots, \lambda_n]}$ is obtained by averaging an ensemble of configurations generated with the current MaxEnt distribution, while $\left\langle \frac{df_j}{d\theta_j} \right\rangle_P$ is evaluated on the real distribution, i.e., the training set. The formal proof of Eq. (8) is reported in Supplementary Materials A 1. Eq. (8) can be implemented with the usual backpropagation by defining an auxiliary cost function \tilde{S}

$$\tilde{S}(\theta_1, \dots, \theta_n) = \frac{1}{N_1} \sum_{i=1}^{N_1} \lambda_i f_i[\theta_1, \dots, \theta_n](x_i) - \frac{1}{N_2} \sum_{i=1}^{N_2} \lambda_i f_i[\theta_1, \dots, \theta_n](\tilde{x}_i), \quad (9)$$

$$\frac{dS}{d\theta_i} = \frac{\partial \tilde{S}}{\partial \theta_i}, \quad (10)$$

where the configurations \tilde{x}_i are sampled through the MaxEnt probability distribution. The gradient of \tilde{S} does not depend explicitly on the probability distribution, therefore, the backpropagation is fast as it does not require running through the ensemble generation. Note that the double optimization of all the θ_i and λ_i parameters works like an adversary competition: the λ_i optimization aims at maximizing entropy with the given set of constraints, while the θ_i optimization alters the set of constraints to minimize the entropy of the distribution, extracting order from disorder. Unlike most machine-learning approaches, the optimization rule in Eq. (8) does not evaluate a distance between the generated data and the training, thus mitigating the risks of overfitting.

In the following sections, we discuss different applications of our approach. First, we focus on a special case where analytical insight can be gained. In particular, we show that Principal component analysis (PCA) can be formally derived from the Min-MaxEnt principle. Next, we probe the capability of the Min-MaxEnt to infer different kinds of 1D bimodal distributions against the predictions of standard MaxEnt and variational autoencoders (VAE). Finally, we apply the method to the contest of image generation, demonstrating (i) its capabilities when trained on a small subset of data, (ii) how it can be refined via adversary network training, and (iii) how controlled generation can be easily enforced on the trained model.

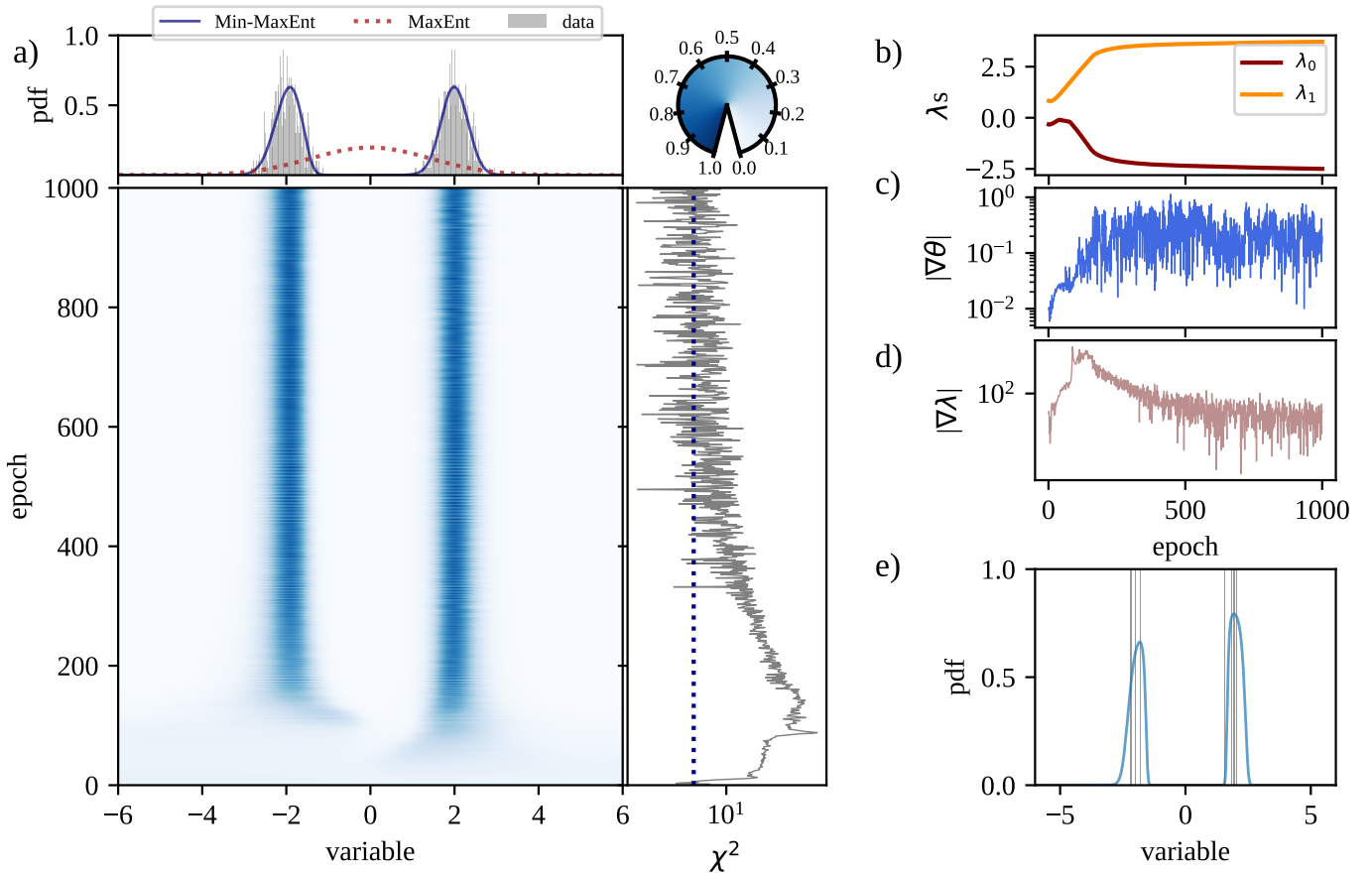


FIG. 3: **Inference of a bimodal normal distribution.** **a)** Inferred Min-MaxEnt distribution as a function of the training epochs for a dataset of 1000 bimodal normal variables. In the top panel, the best-inferred MaxEnt and Min-MaxEnt distributions are reported in red and blue, respectively. Real data distribution is shown in gray. **b)** Values of the Lagrangian multipliers as a function of the training epochs. **c)** Modulus of the gradient of the observables and **d)** Lagrangian multipliers as a function of the training epochs. **e)** Best inferred Min-MaxEnt distributions and real data distribution for a training performed with a dataset composed of 10 samples.

A. Principal component analysis as a special Min-MaxEnt solution

Principal component analysis is a widely used statistical approach to represent high-dimensional data in its essential features or principal components. Such components are obtained by the linear combinations of the original variables that diagonalize the covariance matrix. Due to its capability to reduce dimensionality by retaining only the components with the highest variances, PCA finds wide applications, especially in fields characterized by the presence of vast amounts of data, from bioinformatics [31] to particle physics [32], in tasks like estimating missing values in huge data matrices, sparse component estimation, and the analysis of images, shapes, and functions [33].

In the following, we demonstrate that PCA can be retrieved as a particular solution of the minimal maximum entropy principle by constraining the variance of an arbitrary linear combination of the system variables. Figure 2a) shows a straightforward 2D case in which data

(gray dots) are drawn from a general probability distribution with a covariance matrix $\Sigma_{ij} = \langle x_i x_j \rangle_P$ of elements $\Sigma_{11} = 3$, $\Sigma_{22} = 2$, and $\Sigma_{12} = 1$.

To constrain the variances of a linear combination of the variables, we define the $f_i[\theta](x, y)$ observables as

$$\begin{cases} f_1(x) = (\cos \theta x + \sin \theta y)^2 \\ f_2(x) = (-\sin \theta x + \cos \theta y)^2 \end{cases} \quad (11)$$

The corresponding MaxEnt solution is a normal distribution of the form

$$\tilde{P}[\theta](x, y) \propto \exp \left[\lambda_1 (\cos \theta x + \sin \theta y)^2 + \lambda_2 (-\sin \theta x + \cos \theta y)^2 \right], \quad (12)$$

where the λ_i can be found analytically imposing that the

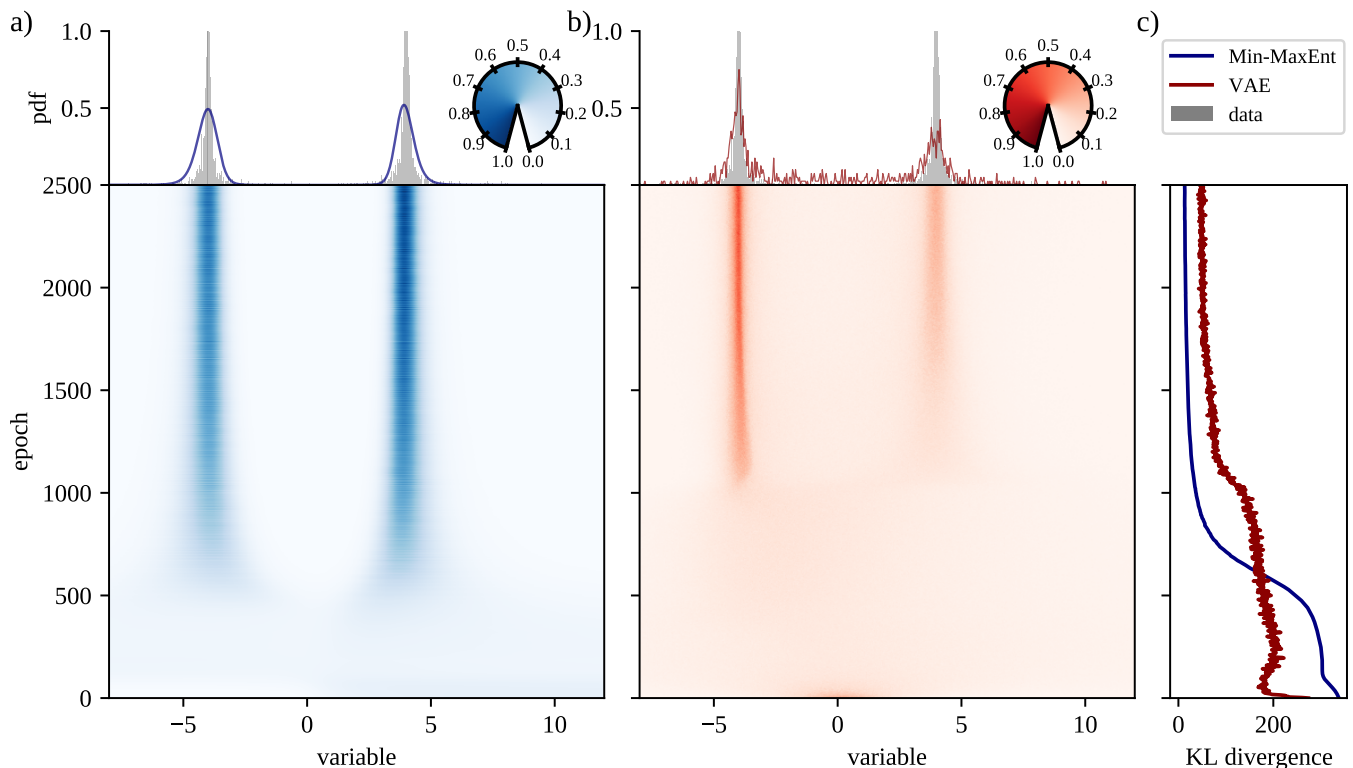


FIG. 4: **Min-MaxEnt vs variational auto-encoder.** a) Inferred Min-MaxEnt distribution as a function of the training epochs for a dataset of 1000 bimodal Lorentians variables. In the top panel, the best-inferred Min-MaxEnt distribution is reported blue, while real data distribution is shown in gray. b) Inferred VAE distribution as a function of the training epochs for a dataset of 1000 bimodal Lorentians variables. In the top panel, the best-inferred VAE distribution is reported red, while real data distribution is shown in gray. c) Kullback–Leibler divergence between real and inferred distributions as a function of the training epochs for the Min-MaxEnt and VAE methods.

averages of $f_i(x)$ matches with the exact distribution:

$$\tilde{\Sigma}_{11} = \frac{1}{2\lambda_1} = \Sigma_{11} \cos^2 \theta + \sin^2 \theta \Sigma_{22} + \Sigma_{12} \sin 2\theta, \quad (13)$$

$$\tilde{\Sigma}_{22} = \frac{1}{2\lambda_2} = \Sigma_{11} \sin^2 \theta + \cos^2 \theta \Sigma_{22} - \Sigma_{12} \sin 2\theta. \quad (14)$$

The entropy of this MaxEnt distribution (Gaussian) is analytical and only depends on the determinant of its covariance matrix, i.e., the product $\tilde{\Sigma}_{11}\tilde{\Sigma}_{22}$

$$S = \frac{1}{2} \ln \left(4\pi^2 e^2 \tilde{\Sigma}_{11} \tilde{\Sigma}_{22} \right). \quad (15)$$

Figure 2b displays the entropy as a function of the rotation angle θ . Minimizing S is equivalent to minimizing the product $\tilde{\Sigma}_{11}\tilde{\Sigma}_{22}$. It can be shown that

$$\tilde{\Sigma}_{11}\tilde{\Sigma}_{22} = \left(\frac{\sin 2\theta}{2} [\Sigma_{11} - \Sigma_{22}] - \cos 2\theta \Sigma_{12} \right)^2 + \text{const}, \quad (16)$$

which is trivially minimized for

$$\theta^* = \frac{1}{2} \arctan \left(\frac{2 \Sigma_{12}}{\Sigma_{11} - \Sigma_{22}} \right) \quad (17)$$

The angle in Eq. (17) also identifies the rotation diagonalizing the real covariance matrix Σ , i.e. the PCA solution. In fact, diagonalizing σ , requires that:

$$\langle (\cos \theta^* x + \sin \theta^* y)(\cos \theta^* y - \sin \theta^* x) \rangle_P = 0. \quad (18)$$

This establishes that the Min-MaxEnt distribution coincides with the PCA solution when the observables f_i are defined as in Eq. (11). In the Supplementary Materials, we generalize this result to arbitrary dimensions, proving that the optimal PCA rotation emerges naturally from minimizing the MaxEnt entropy while constraining variances along an arbitrary basis.

B. Neural network as Min-MaxEnt observables

It is generally challenging to capture complex data patterns with an *ad hoc* parametrization of the observables $f_i(x)$. In this section, we implement the $f_i(x)$ measures as the output layer of a neural network, which parametrizes a general nonlinear function. Specifically, we test the method's performance on a dataset generated from one-dimensional bimodal distributions. First, we draw a set of 1000 training data (see the gray histogram

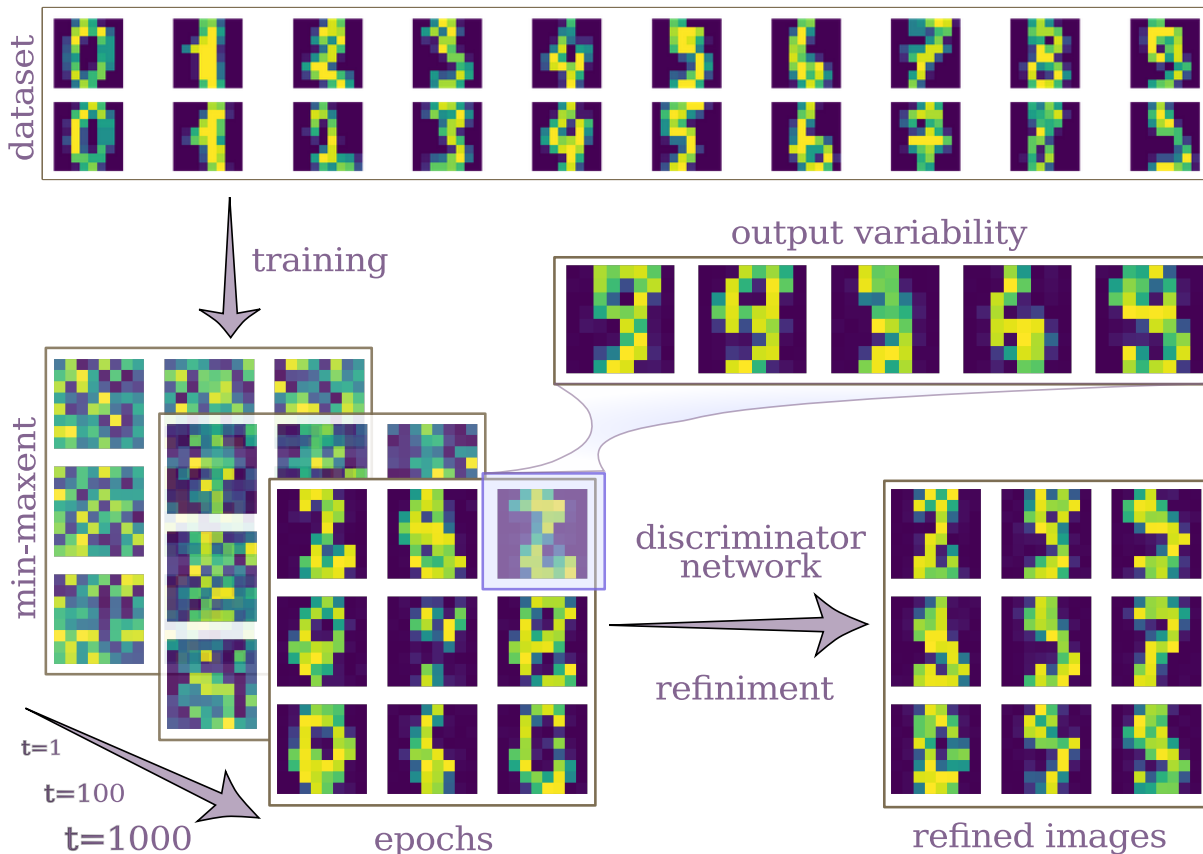


FIG. 5: **Image generation.** Example of the generative power of the proposed Min-MaxEnt principle in the case of images. Starting from the 8x8 MNIST dataset, a Min-MaxEnt is trained using a deep neural network with 16 output observable. The results can be further refined using a discriminator network to bias the generation process.

in the top panel Figure 3a) from a bimodal distribution $P = \frac{1}{2}\mathcal{N}(x, \bar{x}_1, \sigma_1) + \frac{1}{2}\mathcal{N}(x, \bar{x}_2, \sigma_2)$, where \mathcal{N} is a normal distribution with mean \bar{x} and variance σ^2 . Figure 3 shows the results for a Min-MaxEnt run using two observables obtained as output nodes of a multilayer perceptron. Figure 3a displays the evolution of the predicted Min-MaxEnt probability distribution as the training epochs increase. The top panel compares the real data, the Min-MaxEnt distribution after 1000 epochs, and the MaxEnt distribution constraining mean and variance of x . After a few hundred epochs, the Min-MaxEnt distribution perfectly captures both the bimodality and the variances of the single peaks. Notably, the Min-MaxEnt algorithm can infer the distribution without overfitting the data also in the case of scarce input data. Figure 3e displays the inferred Min-MaxEnt distribution (blue) trained only on 10 data points (gray).

A more challenging test is to replace the normal distributions with a Cauchy (Lorentzian) distribution, which allows for rare events to occur far from the distribution peaks. In this case, we compare the Min-MaxEnt with a Variational Autoencoder where the Encoder network has the same architecture as the f_i parametrization (see

Figure 4). The 1000 training data are drawn from the distribution $P(x) = \frac{1}{2}\mathcal{L}(x, x_0^1, \lambda_1) + \frac{1}{2}\mathcal{L}(x, x_0^2, \lambda_2)$, where \mathcal{L} is a Cauchy distribution with median x_0 and half width at half maximum (HWHM) λ . Figure 4a and Figure 4b) display the training of the Min-MaxEnt and VAE, respectively. The final distributions are shown in the top panels with the real data. To quantitatively measure the difference between predicted and real distributions, in Figure 4c, we reported the Kullback-Leibler divergence between real and inferred distributions as a function of the training epochs. The better result of the Min-MaxEnt reflects the tendency of the VAE to overfit rare events, producing a noisy background and overestimating the probability in the regions far from the distribution peaks. This accounts for the notorious issue of VAE, which suffers from blurry generated samples compared to the data they have been trained on [34].

C. Min-MaxEnt for image generation

Next, we applied the Min-MaxEnt algorithm to the case of image generation, using the MNIST dataset [35],

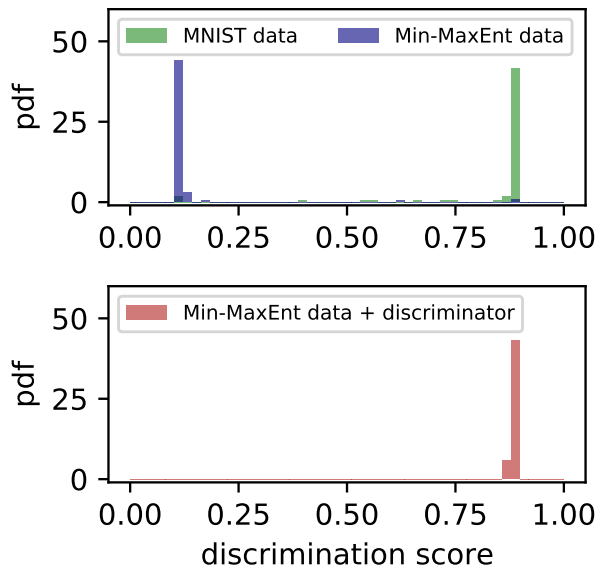


FIG. 6: **Discriminator procedure.** **a)** Probability distribution of the post-training discrimination score for MNIST data (real) and Min-MaxEnt data (generated). **b)** Probability distribution of the post-training discrimination score for data generated via the Min-MaxEnt algorithm with the addition of the discriminator bias.

a collection of 1797 images of greyscale labeled handwritten digits, that are represented as 8x8 pixel matrices. We selected a training set of 200 images, discarding the labels to train the model. The observables are defined through a convolutional neural network (CNN) made by two convolutional layers, tailed by a last fully connected ending in 16 output nodes. The images are generated according to the MaxEnt probability distribution using a Metropolis-Monte Carlo Markov’s chain [28, 29, 36].

The entropy reduction is evident from FIG. 5, where the generative process evolves from noisy images at the first epochs (high entropy) to more defined outputs. Unlike all other generative algorithms, the training procedures never enforce the model’s output to replicate the training set. Therefore, no memory of specific images are stored within the network, preventing overfit and helping with generalization.

Once the model is trained, we have a final probability distribution from which images can be extracted. Consequently, it is possible to define an effective energy landscape for images, which can be further used to direct the generation process:

$$H_0(x) = \sum_{i=1}^{16} f_i[\theta_1 \cdots \theta_n](x) \lambda_i. \quad (19)$$

Similarly to physical systems, generation can be directed by adding an *external field* $H'(x)$. For instance, we can train an independent network $g(x)$ to recognize generated

data like

$$g(x) = \begin{cases} 1 & \text{generated image} \\ 0 & \text{real image} \end{cases} \quad (20)$$

By altering the energy landscape as

$$H(x) = H_0(x) + \underbrace{\alpha g(x)}_{H'(x)}, \quad (21)$$

we can extract biased samples that are guaranteed to be indistinguishable from the original training set according to the network $g(x)$ (see Figure 6). This process can be repeated by updating the training set of the discriminator to include some of the data generated with $H(x)$. Such an approach resembles the adversary network training, which can be applied efficiently to the Min-MaxEnt. In fact, the only network that needs to be re-trained is the discriminator since Eq. (21) automatically generates indistinguishable samples for the respective classifier.

The effective energy landscape framework is also helpful for biasing the generation process toward specific targets. In most GenAI models, this involves some retraining of the network. In contrast, the generation through the Min-MaxEnt algorithm can be conditioned by introducing an external field modeled via a simple CNN classifier. For example, we trained a CNN classifier $h_i(x)$ to guess the labels encoding the written digit of the MNIST dataset (a task extremely easy for networks) like

$$h_i(x) = \begin{cases} 1 & \text{if } x \text{ represents the number } i \\ 0 & \text{otherwise} \end{cases} \quad (22)$$

The biased generation is performed with the new energy landscape as

$$H(x) = H_0(x) - \alpha h_j(x) + \underbrace{\alpha \sum_{i \neq j} h_i(x)}_{H'(x)}. \quad (23)$$

The external field $H'(x)$ favors the generation of images that $h(x)$ classifies as the j number. The result is shown in FIG. 7. The classifier increases the potential energy around numbers different from the target and decreases it around the target. Interestingly, numbers generated via this method appear more readable, as images that cannot be clearly classified as one of the digits are unfavored. The training of $h(x)$ is completely independent of the Min-MaxEnt training, as the only training set employed is the original dataset of real images. Panel d of FIG. 7 shows what happens if we turn off the Min-Max-Ent Hamiltonian, and generate only according to the classifier. In this case, the generative process explores random and noisy configurations where the CNN has no training data, thus entering fake energy minima due to extrapolation.

II. DISCUSSION

Generative artificial intelligence is now permeating everyday life at a pace that has surpassed Moore’s law.

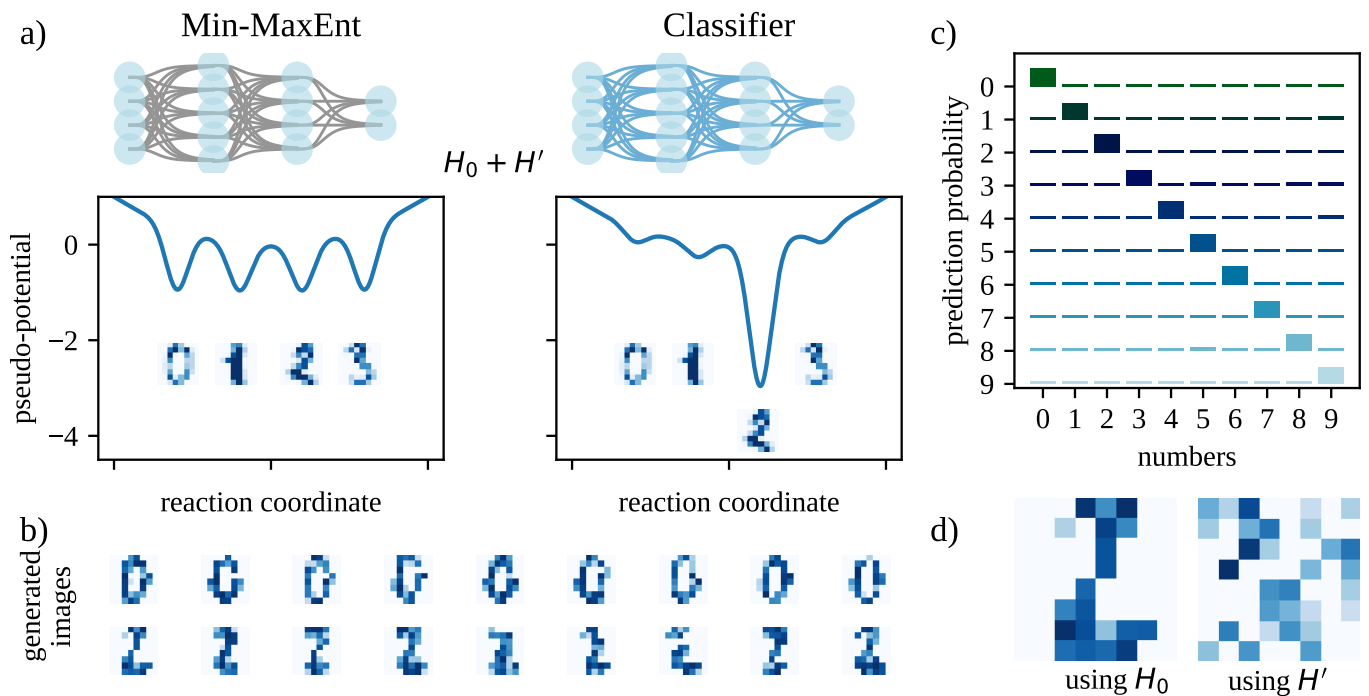


FIG. 7: **Example of preferential-generation process.** **a)** Pictorial representation of the Min-MaxEnt process in MNIST dataset: pseudo-hamiltonian, H_0 , can be interpreted as a pseudo-potential whose minima correspond to different kinds of configurations of the system, i.e., numbers. Adding a classifier neural network as a perturbation H' to H_0 alters the probability of sampling certain kinds of configurations. **b)** Example of biased generations of 0 (top row) and 2 (bottom row). **c)** Classifier capacity of assigning a given configuration to numbers from 0 to 9. **d)** Comparison between a configuration obtained via a Monte Carlo process using only H_0 vs using only H' .

However, while it is being applied to an ever-increasing spectrum of applications, its spread is coupled with some intrinsic flaws, both at the technical and conceptual levels. These comprise, among others, the enormous amount of data needed for the training and the possibility of overfitting to increase performances [14, 15, 18]. Therefore, concerns arise on the persistence of significant progresses in GenAI capabilities, on the ethics/legitimacy of using the generated data, and ultimately, the effective long-term impact of GenAI on society.

The Min-MaxEnt model is a novel generative AI algorithm that differs from most competitors by two significant features: (i) the approach stems from a solid theoretical apparatus rooted in fundamental physics and information theory, (ii) the cost function at the basis of its training never accounts for any metric distance between the generated samples and the training set. As a consequence, the training process is never directly exposed to the training set, thus making it extremely hard for the model to overfit.

The robustness of the Min-MaxEnt to overfit has the promise to lift the concerns regarding copyright violation and fair use of publicly distributed data to train generative models [19, 20]. Indeed, Min-MaxEnt models learn only generalized features/patterns across all the training sets. The approach also proved efficient, compared to state-of-the-art methods, when using small datasets (see

FIG. 3) and/or in the presence of rare events (FIG. 4). Moreover, the ability to control the output via discriminator networks trained *a priori* promotes more effective interaction between the user and the generative process (see FIG. 5 and FIG. 7), currently a significant limitation of most GenAI algorithms. As shown in FIG. 6, the Min-MaxEnt can bypass GenAI detection mechanisms without retraining the model by adding the detection function as a bias in the generative process. While this provides a systematic approach to enhancing the quality of synthetic data, in turn it may raise ethical concerns about the capability of algorithmically distinguishing real from generated content, which could have significant social implications. Therefore, it will be crucial for production applications built on this approach to address these concerns by incorporating watermarks or implementing mechanisms for identifying generated content.

In conclusion, Min-MaxEnt stands out as a first principles approach to GenAI, offering a fundamentally different perspective to the field and enabling to overcome current limitations of state-of-the-art approaches.

Author contributions statement

M.M and L.M. conceived the research, developed the model, wrote and revised the manuscript.

Competing Interests statement

The authors declare no competing financial or non-financial interests.

-
- [1] Zhihan Lv. Generative artificial intelligence in the meta-verse era. *Cognitive Robotics*, 3:208–217, 2023.
- [2] Ashish Vaswani, Noam Shazeer, Niki Parmar, Jakob Uszkoreit, Llion Jones, Aidan N. Gomez, Lukasz Kaiser, and Illia Polosukhin. Attention is all you need. URL <http://arxiv.org/abs/1706.03762>.
- [3] Ian Goodfellow, Jean Pouget-Abadie, Mehdi Mirza, Bing Xu, David Warde-Farley, Sherjil Ozair, Aaron Courville, and Yoshua Bengio. Generative adversarial networks. *Communications of the ACM*, 63(11):139–144, October 2020. ISSN 1557-7317. doi: 10.1145/3422622. URL <http://dx.doi.org/10.1145/3422622>.
- [4] Diederik P. Kingma and Max Welling. auto-encoding variational bayes. URL <http://arxiv.org/abs/1312.6114>.
- [5] Yang Song, Jascha Sohl-Dickstein, Diederik P. Kingma, Abhishek Kumar, Stefano Ermon, and Ben Poole. Score-based generative modeling through stochastic differential equations. 2020.
- [6] Priyanka Gupta, Bosheng Ding, Chong Guan, and Ding Ding. Generative ai: A systematic review using topic modelling techniques. *Data and Information Management*, 8(2):100066, June 2024.
- [7] Kehan Wu, Yingce Xia, Pan Deng, Renhe Liu, Yuan Zhang, Han Guo, Yumeng Cui, Qizhi Pei, Lijun Wu, Shufang Xie, Si Chen, Xi Lu, Song Hu, Jinzhi Wu, Chi-Kin Chan, Shawn Chen, Liangliang Zhou, Nenghai Yu, Enhong Chen, Haiguang Liu, Jinjiang Guo, Tao Qin, and Tie-Yan Liu. Tamgen: drug design with target-aware molecule generation through a chemical language model. *Nature Communications*, 15(1), October 2024.
- [8] Amit Gangwal, Azim Ansari, Iqar Ahmad, Abul Kalam Azad, Vinod Kumarasamy, Vetrivelan Subramaniyan, and Ling Shing Wong. Generative artificial intelligence in drug discovery: basic framework, recent advances, challenges, and opportunities. *Frontiers in Pharmacology*, 15, February 2024.
- [9] Jeanne Trinquier, Guido Uguzzoni, Andrea Pagnani, Francesco Zamponi, and Martin Weigt. Efficient generative modeling of protein sequences using simple autoregressive models. *Nature Communications*, 12(1), October 2021.
- [10] Claudio Zeni, Robert Pinsler, Daniel Zügner, Andrew Fowler, Matthew Horton, Xiang Fu, Zilong Wang, Aleksandra Shysheya, Jonathan Crabbé, Shoko Ueda, Roberto Sordillo, Lixin Sun, Jake Smith, Bichlien Nguyen, Hannes Schulz, Sarah Lewis, Chin-Wei Huang, Ziheng Lu, Yichi Zhou, Han Yang, Hongxia Hao, Jielan Li, Chunlei Yang, Wenjie Li, Ryota Tomioka, and Tian Xie. A generative model for inorganic materials design. *Nature*, January 2025.
- [11] Ketan Totlani. The evolution of generative ai: Implications for the media and film industry. *International Journal for Research in Applied Science and Engineering Technology*, 11(10):973–980, October 2023.
- [12] Locky Law. Application of generative artificial intelligence (genai) in language teaching and learning: A scoping literature review. *Computers and Education Open*, 6: 100174, June 2024.
- [13] Konstantinos I. Roumeliotis and Nikolaos D. Tselikas. Chatgpt and open-ai models: A preliminary review. *Future Internet*, 15(6):192, May 2023.
- [14] Nicolas Carlini, Jamie Hayes, Milad Nasr, Matthew Jagielski, Vikash Sehwal, Florian Tramèr, Borja Balle, Daphne Ippolito, and Eric Wallace. Extracting training data from diffusion models. In *32nd USENIX Security Symposium (USENIX Security 23)*, pages 5253–5270, Anaheim, CA, August 2023. USENIX Association. ISBN 978-1-939133-37-3. URL <https://www.usenix.org/conference/usenixsecurity23/presentation/carlini>.
- [15] Nicola Jones. The ai revolution is running out of data. what can researchers do? *Nature*, 636(8042):290–292, December 2024. doi: 10.1038/d41586-024-03990-2.
- [16] Ilya Shumailov, Zakhar Shumaylov, Yiren Zhao, Nicolas Papernot, Ross Anderson, and Yarin Gal. Ai models collapse when trained on recursively generated data. *Nature*, 631(8022):755–759, July 2024.
- [17] Sina Alemohammad, Josue Casco-Rodriguez, Lorenzo Luzi, Ahmed Intiaz Humayun, Hossein Babaei, Daniel LeJeune, Ali Siahkoobi, and Richard G. Baraniuk. Self-consuming generative models go mad. 2023.
- [18] Daphne Ippolito, Florian Tramèr, Milad Nasr, Chiyuan Zhang, Matthew Jagielski, Katherine Lee, Christopher A Choquette-Choo, and Nicholas Carlini. Preventing verbatim memorization in language models gives a false sense of privacy. *arXiv preprint arXiv:2210.17546*, 2022.
- [19] Zachary Small. Sarah silverman sues openai and meta over copyright infringement. *The New York Times*, pages Sec. C, 3, July 2023. URL <https://www.nytimes.com/2023/07/10/arts/sarah-silverman-lawsuit-openai-meta.html>.
- [20] Jocelyn Dzuong, Zichong Wang, and Wenbin Zhang. Uncertain boundaries: Multidisciplinary approaches to copyright issues in generative ai. *arXiv preprint arXiv:2404.08221*, 2024.
- [21] Ming Li, Taojiannan Yang, Huafeng Kuang, Jie Wu, Zhaoning Wang, Xuefeng Xiao, and Chen Chen. ControlNet++: Improving conditional controls with efficient consistency feedback. URL <http://arxiv.org/abs/2404.07987>.
- [22] Lianghua Huang, Di Chen, Yu Liu, Yujun Shen, Deli Zhao, and Jingren Zhou. Composer: Creative and controllable image synthesis with composable conditions. *arXiv preprint arXiv:2302.09778*, 2023.
- [23] Lvmin Zhang, Anyi Rao, and Maneesh Agrawala. Adding conditional control to text-to-image diffusion models. URL <http://arxiv.org/abs/2302.05543>.
- [24] Edward J. Hu, Yelong Shen, Phillip Wallis, Zeyuan Allen-Zhu, Yuanzhi Li, Shean Wang, Lu Wang, and Weizhu Chen. LoRA: Low-rank adaptation of large

- language models. URL <http://arxiv.org/abs/2106.09685>.
- [25] Shaoran Xie, Zhifei Zhang, Zhe Lin, Tobias Hinz, and Kun Zhang. Smartbrush: Text and shape guided object inpainting with diffusion model. In *Proceedings of the IEEE/CVF Conference on Computer Vision and Pattern Recognition*, pages 22428–22437, 2023.
- [26] Robin Rombach, Andreas Blattmann, Dominik Lorenz, Patrick Esser, and Björn Ommer. High-resolution image synthesis with latent diffusion models. In *Proceedings of the IEEE/CVF conference on computer vision and pattern recognition*, pages 10684–10695, 2022.
- [27] William Bialek. *Biophysics*. Princeton University Press, Princeton, NJ, October 2012.
- [28] Mattia Miotto and Lorenzo Monacelli. Entropy evaluation sheds light on ecosystem complexity. *Phys. Rev. E*, 98:042402, Oct 2018.
- [29] Mattia Miotto and Lorenzo Monacelli. TOLOMEO, a Novel Machine Learning Algorithm to Measure Information and Order in Correlated Networks and Predict Their State. *Entropy*, 23(9):1138, September 2021. Number: 9 Publisher: Multidisciplinary Digital Publishing Institute.
- [30] Diederik P. Kingma and Jimmy Ba. Adam: A method for stochastic optimization. *CoRR*, abs/1412.6980, 2014. URL <https://api.semanticscholar.org/CorpusID:6628106>.
- [31] S. Ma and Y. Dai. Principal component analysis based methods in bioinformatics studies. *Briefings in Bioinformatics*, 12(6):714–722, January 2011.
- [32] I. Altsybeev. Application of principal component analysis to establish a proper basis for flow studies in heavy-ion collisions. *Physics of Particles and Nuclei*, 51(3):314–318, May 2020.
- [33] Michael Greenacre, Patrick J. F. Groenen, Trevor Hastie, Alfonso Iodice D’Enza, Angelos Markos, and Elena Tuzhilina. Principal component analysis. *Nature Reviews Methods Primers*, 2(1), December 2022.
- [34] Gustav Bredell, Kyriakos Flouris, Krishna Chaitanya, Ertunc Erdil, and Ender Konukoglu. Explicitly minimizing the blur error of variational autoencoders. 2023.
- [35] C. Kaynak E. Alpaydin. Optical recognition of hand-written digits. 1998. doi: 10.24432/C50P49. URL <https://archive.ics.uci.edu/dataset/80>.
- [36] W. K. Hastings. Monte carlo sampling methods using markov chains and their applications. *Biometrika*, 57(1): 97–109, April 1970.

Supplementary Materials A: Methods

1. Total derivative of the entropy

Consider a probability distribution of the form $P = \frac{e^{-\beta H}}{Z}$ with $Z = \int dx e^{-\beta H}$, where is given by $H = \sum_i \lambda_i f_i$, i.e. is the sum of N observable, $\{f_i\}_N$ each multiplied by its Lagrangian multiplier, $\{\lambda_i\}_N$ and assume that the observables (and in turn the multipliers) are function of a set of parameters, $\{\theta_\rho\}_M$. The entropy of such system is given by $S(\theta, \lambda(\theta) = - \int dx P \ln(P)$

The total derivative of the entropy with respect to the parameters of the observables is given by:

$$\frac{dS}{d\theta_\rho} = \frac{\partial S}{\partial \theta_\rho} + \sum_i \frac{\partial S}{\partial \lambda_i} \frac{d\lambda_i}{d\theta_\rho} \quad (\text{A1})$$

where we have that:

$$\frac{\partial S}{\partial \theta_\rho} = \frac{\partial}{\partial \theta_\rho} \left[- \int dx P \ln(P) \right] = \frac{\partial}{\partial \theta_\rho} \left[- \int dx P [-\beta H - \ln(Z)] \right] = \beta \frac{\partial \langle H \rangle_P}{\partial \theta_\rho} + \frac{\partial \ln(Z)}{\partial \theta_\rho} \quad (\text{A2})$$

Using the relation: $\frac{\partial \ln Z}{\partial \theta_\rho} = \frac{\partial Z}{\partial \theta_\rho} / Z = \int dx P \frac{\partial H}{\partial \theta_\rho} = -\beta \langle \frac{\partial H}{\partial \theta_\rho} \rangle$, we get to:

$$\frac{\partial S}{\partial \theta_\rho} = -\beta \left(\left\langle \frac{\partial H}{\partial \theta_\rho} \right\rangle_P - \frac{\partial \langle H \rangle_P}{\partial \theta_\rho} \right) \quad (\text{A3})$$

where $\langle \cdot \rangle_P$, indicates the average over the probability distribution, P .

This equation in turn can be written as:

$$\frac{\partial S}{\partial \theta_\rho} = -\beta \left(\left\langle \frac{\partial H}{\partial \theta_\rho} \right\rangle_P - \int dx \frac{\partial H}{\partial \theta_\rho} P - \int dx \frac{\partial P}{\partial \theta_\rho} H \right) \quad (\text{A4})$$

that reduces to:

$$\frac{\partial S}{\partial \theta_\rho} = +\beta \left\langle \sum_i \lambda_i f_i \frac{\partial \ln P}{\partial \theta_\rho} \right\rangle \quad (\text{A5})$$

The above equation can be further solved to yield:

$$\frac{\partial S}{\partial \theta_\rho} = -\beta \left\langle \sum_i \lambda_i f_i \right\rangle \frac{\partial \ln Z}{\partial \theta_\rho} - \beta^2 \sum_{ij} \lambda_i \lambda_j \left\langle f_i \frac{df_j}{d\theta_\rho} \right\rangle \quad (\text{A6})$$

where

$$\frac{\partial \ln Z}{\partial \theta_\rho} = -\beta \left\langle \sum_i \lambda_i \frac{df_i}{d\theta_\rho} \right\rangle \quad (\text{A7})$$

Plugging all terms together, the final expression of $\frac{\partial S}{\partial \theta_\rho}$ becomes:

$$\frac{\partial S}{\partial \theta_\rho} = -\beta^2 \sum_{ij} \lambda_i \lambda_j \left(\left\langle f_i \frac{df_j}{d\theta_\rho} \right\rangle - \langle f_i \rangle \left\langle \frac{df_j}{d\theta_\rho} \right\rangle \right) \quad (\text{A8})$$

The second term of Eq. A1 instead is given by two contributions. In particular, the term $\frac{\partial S}{\partial \lambda}$ assume the same formal expression of Eq. A3:

$$\frac{\partial S}{\partial \lambda_i} = -\beta \left(\left\langle \frac{\partial H}{\partial \lambda_i} \right\rangle_P - \frac{\partial \langle H \rangle_P}{\partial \lambda_i} \right) = -\beta \left(\langle f_i \rangle - \frac{\partial}{\partial \lambda_i} \langle H \rangle \right) \quad (\text{A9})$$

This can be written as

$$\frac{\partial S}{\partial \lambda_i} = -\beta \left[\langle f_i \rangle - \frac{\partial}{\partial \lambda_i} \int dx \left(\sum_j \lambda_j f_j \right) P(\lambda, x) \right] = -\beta \left[\langle f_i \rangle - \int dx \left(\sum_j \lambda_j f_j \right) \frac{\partial P}{\partial \lambda_i} - \int dx f_i P \right] \quad (\text{A10})$$

which simplifies in:

$$\frac{\partial S}{\partial \lambda_i} = +\beta \left\langle \left(\sum_j \lambda_j f_j \right) \frac{\partial \ln P}{\partial \lambda_i} \right\rangle \quad (\text{A11})$$

The logarithm of the probability distribution is given by:

$$\ln P = -\beta \sum_i \lambda_i f_i - \ln \left(\int dx e^{-\beta \sum_i \lambda_i f_i} \right)$$

Thus the derivative of this term with respect to the i-th Lagrangian multiplier assumes the form:

$$\frac{\partial \ln P}{\partial \lambda_i} = -\beta f_i - \int dx \frac{-\beta f_i e^{-\sum_k \beta \lambda_k f_k}}{Z} = -\beta (f_i - \langle f_i \rangle) \quad (\text{A12})$$

Plugging all terms together, we obtain:

$$\frac{\partial S}{\partial \lambda_j} = -\beta^2 \left\langle \left(\sum_i \lambda_i f_i \right) (f_j - \langle f_j \rangle) \right\rangle \quad (\text{A13})$$

Noting that:

$$\langle f_i (f_j - \langle f_j \rangle) \rangle - \underbrace{\langle \langle f_i \rangle (f_j - \langle f_j \rangle) \rangle}_{=0} = \langle (f_i - \langle f_i \rangle) (f_j - \langle f_j \rangle) \rangle$$

we get to the final expression:

$$\frac{\partial S}{\partial \lambda_j} = -\beta^2 \sum_i \lambda_i (\Sigma_{\text{MC}})_{ij} \quad (\text{A14})$$

with Σ_{MC} being the covariance matrix computed on the configurations.

Finally, to get an expression for the derivative of the Lagrangian multiplier with respect to the observable, we need to adopt a perturbation approach ($H \rightarrow H + \delta H$). In this framework, we have that $H' = H_0 + \sum_i d\lambda_i f_i + \lambda_i df_i$ and assume that $\langle f_i \rangle_{H'} = \langle f_i \rangle_P$.

Computing the average of an observable over configurations generated by H' equals to:

$$\langle f_i \rangle_H = \langle f_i + df_i \rangle_{H_0 + \delta H}$$

The probability distribution terms become:

$$e^{-\beta H'} = e^{-\beta H_0} e^{-\beta \sum_i d\lambda_i f_i} e^{-\beta \sum_i \lambda_i df_i} \quad (\text{A15})$$

and since the perturbation is small and linear, we have:

$$e^{-\beta H'} \simeq e^{-\beta H_0} \left(1 - \beta \sum_i (d\lambda_i f_i + \lambda_i df_i) \right) \quad (\text{A16})$$

The partition function is given by:

$$Z' = \int dx e^{-\beta H'} = \int dx e^{-\beta H_0} \left(1 - \beta \sum_i (d\lambda_i f_i + \lambda_i df_i) \right) \quad (\text{A17})$$

which can be recast into

$$\frac{Z'}{Z_0} = 1 - \beta \sum_i (d\lambda_i \langle f_i \rangle + \lambda_i \langle df_i \rangle) \quad (\text{A18})$$

It follows that:

$$\langle f_i + df_i \rangle_{H'} = \int [f_i + df_i] \frac{e^{-\beta H'} Z_0}{Z' Z_0} = \int [f_i + df_i] \frac{1 - \beta \sum_i (d\lambda_i f_i + \lambda_i df_i)}{1 - \beta \sum_i (d\lambda_i \langle f_i \rangle + \lambda_i \langle df_i \rangle)} \frac{e^{-\beta H_0}}{Z_0} \quad (\text{A19})$$

Keeping again only the first-order terms, we have:

$$\langle f_i + df_i \rangle_{H'} = \langle df_i \rangle_{H_0} - \beta \sum_j (d\lambda_j \langle f_i f_j \rangle + \lambda_j \langle df_j f_i \rangle) + \beta \langle f_i \rangle \sum_j (d\lambda_j \langle f_j \rangle + \lambda_j \langle df_j \rangle) \quad (\text{A20})$$

We must now impose that

$$\langle f_i + df_i \rangle_{H'} = \langle f_i + df_i \rangle_P \quad (\text{A21})$$

Keeping only the first order term in both, we have

$$\langle df_i \rangle_P = \langle df_i \rangle_{H_0} - \beta \sum_j (d\lambda_j \langle f_i f_j \rangle + \lambda_j \langle df_j f_i \rangle) + \beta \langle f_i \rangle \sum_j (d\lambda_j \langle f_j \rangle + \lambda_j \langle df_j \rangle) \quad (\text{A22})$$

$$\langle df_j \rangle_P - \langle df_j \rangle_{H_0} = -\beta \sum_i \lambda_i (\langle f_j df_i \rangle - \langle f_j \rangle \langle df_i \rangle) - \beta \sum_i d\lambda_i (\langle f_j f_i \rangle - \langle f_j \rangle \langle f_i \rangle) \quad (\text{A23})$$

We can define the covariance matrix with respect to the H_0 distribution as

$$\Sigma_{ij}^{\text{MC}} = \langle f_i f_j \rangle_{H_0} - \langle f_i \rangle_{H_0} \langle f_j \rangle_{H_0} \quad (\text{A24})$$

and reorganize terms in equation A23 to get

$$\langle df_j \rangle_P - \langle df_j \rangle_{H_0} = -\beta \sum_i \lambda_i (\langle f_j df_i \rangle - \langle f_j \rangle \langle df_i \rangle) - \beta \sum_i d\lambda_i \Sigma_{ij}^{\text{MC}} \quad (\text{A25})$$

and

$$\sum_i d\lambda_i \Sigma_{ij}^{\text{MC}} = \frac{\langle df_j \rangle_{H_0} - \langle df_j \rangle_P}{\beta} - \sum_i \lambda_i (\langle f_j df_i \rangle_{H_0} - \langle f_j \rangle_{H_0} \langle df_i \rangle_{H_0}) \quad (\text{A26})$$

Inverting the relation, we get the response function

$$d\lambda_i = \frac{1}{\beta} \sum_j (\Sigma_{\text{MC}}^{-1})_{ij} (\langle df_j \rangle_{H_0} - \langle df_j \rangle_P) - \sum_{jk} \lambda_k (\Sigma_{\text{MC}}^{-1})_{ij} (\langle f_j df_k \rangle_{H_0} - \langle f_j \rangle_{H_0} \langle df_k \rangle_{H_0}) \quad (\text{A27})$$

We can differentiate with respect to the parameter:

$$\frac{d\lambda_i}{d\theta_\rho} = \frac{1}{\beta} \sum_j (\Sigma_{\text{MC}}^{-1})_{ij} \left(\left\langle \frac{df_j}{d\theta_\rho} \right\rangle_{H_0} - \left\langle \frac{df_j}{d\theta_\rho} \right\rangle_P \right) - \sum_{jk} \lambda_k (\Sigma_{\text{MC}}^{-1})_{ij} \left(\left\langle f_j \frac{df_k}{d\theta_\rho} \right\rangle_{H_0} - \langle f_j \rangle_{H_0} \left\langle \frac{df_k}{d\theta_\rho} \right\rangle_{H_0} \right) \quad (\text{A28})$$

The second term of Eq. A1 can now be composed as

$$\sum_i \frac{\partial S}{\partial \lambda_i} \frac{d\lambda_i}{d\theta_\rho} = -\beta \sum_h \lambda_h \sum_j \delta_{hj} \left(\left\langle \frac{df_j}{d\theta_\rho} \right\rangle_{H_0} - \left\langle \frac{df_j}{d\theta_\rho} \right\rangle_P \right) + \beta^2 \sum_h \lambda_h \sum_{jk} \delta_{hj} \lambda_k \left(\left\langle f_j \frac{df_k}{d\theta_\rho} \right\rangle_{H_0} - \langle f_j \rangle_{H_0} \left\langle \frac{df_k}{d\theta_\rho} \right\rangle_{H_0} \right) \quad (\text{A29})$$

where the Kronecker δ s arises from the multiplication of the covariance matrix with its inverse. Simplifying the indexes, the expression assumes the form:

$$\sum_i \frac{\partial S}{\partial \lambda_i} \frac{d\lambda_i}{d\theta_\rho} = -\beta \sum_h \lambda_h \left(\left\langle \frac{df_h}{d\theta_\rho} \right\rangle_{H_0} - \left\langle \frac{df_h}{d\theta_\rho} \right\rangle_P \right) + \underbrace{\beta^2 \sum_h \lambda_h \sum_k \lambda_k \left(\left\langle f_h \frac{df_k}{d\theta_\rho} \right\rangle_{H_0} - \langle f_h \rangle_{H_0} \left\langle \frac{df_k}{d\theta_\rho} \right\rangle_{H_0} \right)}_{= -\frac{\partial S}{\partial \theta_\rho}} \quad (\text{A30})$$

The final expression for the total derivative of the entropy is

$$\frac{dS}{d\theta_\rho} = -\beta \sum_h \lambda_h \left(\left\langle \frac{df_h}{d\theta_\rho} \right\rangle_{H_0} - \left\langle \frac{df_h}{d\theta_\rho} \right\rangle_P \right) \quad (\text{A31})$$

2. Principal component analysis as MinMax Ent solution of variable linear combinations

Here, we provide the detailed proof that PCA is a special solution of the minimal maximum entropy principle using as constraints/observables the squares of linear combinations of the system variables.

Let us assume that the system real probability distribution is characterized by a covariance matrix, Σ , and null n -dimensional vector of the mean values, $\bar{\mu} = 0$.

a. *Two dimensional case*

To begin with, we start considering the two-dimensional case assuming that $\vec{\mu} = 0$ (this condition can always be achieved simply translating the system variables). Next, we define the observables as $f_i = y_i^2 = \left(\sum_j^n \theta_j x_j\right)^2$, i.e. as the variance of the linear combination of the system variables.

In this case, it is easy to show that the maximum entropy distribution is a normal distribution of the form:

$$\tilde{P} = \frac{e^{\sum_i \lambda_i y_i^2}}{Z} = \frac{e_0^H}{Z} \quad (\text{A32})$$

with $\lambda_i = -\frac{1}{2\langle y_i^2 \rangle_P}$, which depend on the set of $\{\theta_i\}$ parameters. We have now restrained the probability space to the region that maximizes entropy with respect to the constraints. Now one could ask what are the values of the parameters that yield the minimum entropy in this region. In other words, we want to solve the system:

$$\frac{dS}{d\theta_i} = 0 \quad (\text{A33})$$

To begin with, let us start with the 2D case, where data can be easily represented as the scatter plot in Figure 2. In the 2D case, we have that:

$$\bar{y} = \begin{bmatrix} y_1 \\ y_2 \end{bmatrix} = \Theta \begin{bmatrix} x_1 \\ x_2 \end{bmatrix} \quad \text{with} \quad \Theta = \begin{bmatrix} \theta_{11} & \theta_{12} \\ \theta_{21} & \theta_{22} \end{bmatrix} \quad (\text{A34})$$

Imposing, without loosing generality, that the linear combination is a rotation, equals to requiring that $\Theta\Theta^T = I$. The relationship is satisfied by a matrix of the form:

$$\Theta = \frac{1}{\sqrt{\alpha^2 + \beta^2}} \begin{bmatrix} \alpha & -\beta \\ \beta & \alpha \end{bmatrix} \quad (\text{A35})$$

We can now use expression 8 to find the values of the parameters:

$$\frac{dS}{d\alpha} = \lambda_1 \left(\left\langle 2y_1 \frac{\partial y_1}{\partial \alpha} \right\rangle_{H_0} - \left\langle 2y_1 \frac{\partial y_1}{\partial \alpha} \right\rangle_P \right) + \lambda_2 \left(\left\langle 2y_2 \frac{\partial y_2}{\partial \alpha} \right\rangle_{H_0} - \left\langle 2y_2 \frac{\partial y_2}{\partial \alpha} \right\rangle_P \right) = 0 \quad (\text{A36})$$

while the second term is given by:

$$\frac{dS}{d\beta} = \lambda_1 \left(\left\langle 2y_1 \frac{\partial y_1}{\partial \beta} \right\rangle_{H_0} - \left\langle 2y_1 \frac{\partial y_1}{\partial \beta} \right\rangle_P \right) + \lambda_2 \left(\left\langle 2y_2 \frac{\partial y_2}{\partial \beta} \right\rangle_{H_0} - \left\langle 2y_2 \frac{\partial y_2}{\partial \beta} \right\rangle_P \right) = 0 \quad (\text{A37})$$

From Eq. A34, we can compute the term $\partial y_i / \partial \alpha$ and $\partial y_i / \partial \beta$ as:

$$\begin{cases} \frac{\partial y_1}{\partial \alpha} = \frac{x_1}{\sqrt{\alpha^2 + \beta^2}} - y_1 \frac{\alpha}{\alpha^2 + \beta^2} = \frac{\beta y_2}{\alpha^2 + \beta^2} \\ \frac{\partial y_1}{\partial \beta} = -\frac{x_2}{\sqrt{\alpha^2 + \beta^2}} - y_1 \frac{\beta}{\alpha^2 + \beta^2} = -\frac{\alpha y_2}{\alpha^2 + \beta^2} \\ \frac{\partial y_2}{\partial \alpha} = \frac{x_2}{\sqrt{\alpha^2 + \beta^2}} - y_2 \frac{\alpha}{\alpha^2 + \beta^2} = -\frac{\beta y_1}{\alpha^2 + \beta^2} \\ \frac{\partial y_2}{\partial \beta} = \frac{x_1}{\sqrt{\alpha^2 + \beta^2}} - y_2 \frac{\beta}{\alpha^2 + \beta^2} = \frac{\alpha y_1}{\alpha^2 + \beta^2} \end{cases} \quad (\text{A38})$$

where we used the inverse relation:

$$\bar{x} = \begin{bmatrix} x_1 \\ x_2 \end{bmatrix} = \frac{1}{\sqrt{\alpha^2 + \beta^2}} \begin{bmatrix} \alpha & \beta \\ -\beta & \alpha \end{bmatrix} \bar{y} \quad (\text{A39})$$

Substituting the expressions for the derivatives in Eq. A36, one gets to:

$$\frac{dS}{d\alpha} = \lambda_1 \frac{2\beta}{\alpha^2 + \beta^2} (\langle y_1 y_2 \rangle_{H_0} - \langle y_1 y_2 \rangle_P) - \lambda_2 \frac{2\beta}{\alpha^2 + \beta^2} (\langle y_1 y_2 \rangle_{H_0} - \langle y_1 y_2 \rangle_P) = 0 \quad (\text{A40})$$

Simplifying the notation and noting that $\langle y_1 y_2 \rangle_{H_0} = 0$, one get to the final expression:

$$(\lambda_1 - \lambda_2) \langle y_1 y_2 \rangle_P = 0 \quad (\text{A41})$$

The previous expression can be satisfied in the trivial case in which the two Lagrangian multipliers are the same or by a linear combination of the variables such that:

$$\langle y_1 y_2 \rangle_P = \alpha \beta (\langle x_1 x_1 \rangle_P - \langle x_2 x_2 \rangle_P) + \langle x_1 x_2 \rangle_P (\alpha^2 + \beta^2) = 0 \quad (\text{A42})$$

b. Principal component transformation

To get the meaning of Eq. A42, we can go through the simple calculation of the 2D PCA transformation. Given a 2D covariance matrix, the PCA transformation equals to find the basis that diagonalizes the covariance matrix, i.e.

$$U \Sigma U^t = \frac{1}{\sqrt{\alpha^2 + \beta^2}} \begin{bmatrix} \alpha & -\beta \\ \beta & \alpha \end{bmatrix} \begin{bmatrix} \langle x_1 x_1 \rangle_P & \langle x_1 x_2 \rangle_P \\ \langle x_1 x_2 \rangle_P & \langle x_2 x_2 \rangle_P \end{bmatrix} \frac{1}{\sqrt{\alpha^2 + \beta^2}} \begin{bmatrix} \alpha & \beta \\ -\beta & \alpha \end{bmatrix} = \begin{bmatrix} \tilde{\lambda}_1 & 0 \\ 0 & \tilde{\lambda}_1 \end{bmatrix} \quad (\text{A43})$$

where the U matrix is written in such a way that the two columns are linearly independent, while each column correspond to a normalized vector. Note that this results in the same format Eq. A34. A straightforward calculation leads to recast Eq. A43 as:

$$\begin{bmatrix} \langle y_1 y_1 \rangle_P & \langle y_1 y_2 \rangle_P \\ \langle y_1 y_2 \rangle_P & \langle y_2 y_2 \rangle_P \end{bmatrix} = \begin{bmatrix} \tilde{\lambda}_1 & 0 \\ 0 & \tilde{\lambda}_1 \end{bmatrix} \quad (\text{A44})$$

which proves that fulfilling relation Eq. A42 equals to finding the PCA transformation.

c. N-dimensional case

To demonstrate the validity of the previous result in a n-dimensional case, we proceed by induction: we assume that it is true in n-1 dimension and show it works in n dimension. If the relation holds for n-1, it means we can rotate the system in such a way that the observable linear combination matrix has the form:

$$\bar{y} = \underbrace{\begin{pmatrix} \alpha_1 & 0 & \dots & \dots & 0 & \delta_1 \\ 0 & \alpha_2 & 0 & \dots & 0 & \delta_2 \\ 0 & 0 & \alpha_i & 0 & 0 & \delta_i \\ 0 & \dots & 0 & \alpha_{n-1} & \delta_{n-1} \\ \beta_1 & \dots & \beta_i & \dots & \beta_{n-1} & \gamma \end{pmatrix}}_{\Theta} \bar{x} \quad (\text{A45})$$

Imposing that $\Theta \Theta^t = I$, as done in the 2D case, equals to:

$$\begin{pmatrix} \alpha_1 & 0 & \dots & \dots & 0 & \delta_1 \\ 0 & \alpha_2 & 0 & \dots & 0 & \delta_2 \\ 0 & 0 & \alpha_i & 0 & 0 & \delta_i \\ 0 & \dots & 0 & \alpha_{n-1} & \delta_{n-1} \\ \beta_1 & \dots & \beta_i & \dots & \beta_{n-1} & \gamma \end{pmatrix} \begin{pmatrix} \alpha_1 & 0 & \dots & \dots & 0 & \beta_1 \\ 0 & \alpha_2 & 0 & \dots & 0 & \beta_2 \\ 0 & 0 & \alpha_i & 0 & 0 & \beta_i \\ 0 & \dots & 0 & \alpha_{n-1} & \beta_{n-1} \\ \delta_1 & \dots & \delta_i & \dots & \delta_{n-1} & \gamma \end{pmatrix} = \\ = \begin{pmatrix} \alpha_1^2 + \delta_1^2 & \delta_1 \delta_2 & \dots & \delta_1 \delta_j & \dots & \beta_1 \alpha_1 + \delta_1 \gamma \\ \delta_1 \delta_2 & \alpha_2^2 + \delta_2^2 & \dots & \dots & \dots & \dots \\ \dots & \dots & \alpha_i^2 + \delta_i^2 & \dots & \dots & \dots \\ \dots & \dots & \dots & \dots & \alpha_{n-1}^2 + \delta_{n-1}^2 & \beta_{n-1} \alpha_{n-1} + \delta_{n-1} \gamma \\ \beta_1 \alpha_1 + \delta_1 \gamma & \dots & \dots & \dots & \beta_{n-1} \alpha_{n-1} + \delta_{n-1} \gamma & \sum_i \beta_i^2 + \gamma^2 \end{pmatrix} = I \quad (\text{A46})$$

Since the α_i can not be null, in order for this expression to be satisfied, $\delta_i = 0$ for $i \in (1, n-2)$, $\beta_i = 0$ for $i \in (1, n-2)$, and $\alpha_i = 1$ for $i \in (1, n-2)$. Thus, the problem reduces to a two dimensional case, as only the α_{n-1} , δ_{n-1} , β_{n-1} and γ parameters remain to be determined. But we already proved in the previous section that the PCA rotation is equivalent to the minimal maximum entropy one in a two dimensional case, so it follows that the result is true for n-dimensional data.